Packing Spheres Tightly: Influence of Mechanical Stability on Close-Packed Sphere Structures

S. Heitkam,[1,2] W. Drenckhan,[1] and J. Fröhlich[2]

[1]*Laboratoire de Physique des Solides—UMR 8502, Université Paris Sud, 91405 Orsay, France*
[2]*Institut für Strömungsmechanik, Technische Universität Dresden, 01069 Dresden, Germany*

(Received 8 December 2011; published 5 April 2012)

Many experiments and simulations of packings of monodisperse hard spheres report a dominance of the face-centered cubic structure in the hexagonally close-packed limit, even though it has no significant energetic or entropic gain over other close-packed configurations. Combining simulations and experiments, we demonstrate that a simple mechanical instability which occurs during the packing process may play an important role in selecting the face-centered cubic structure over other close-packed alternatives. Our argument is supported by detailed quantitative analyses of key configurations in sphere packings and highlights the importance of the packing dynamics. The proposed mechanism is elementary and should therefore play a role in a wide range of sphere systems.

DOI: 10.1103/PhysRevLett.108.148302 PACS numbers: 82.70.−y, 45.70.−n, 47.55.D−, 61.50.Ah

Understanding how spheres pack together is an art as much as a science [1] and has kept generations of physicists, mathematicians, and engineers on their toes. Sphere packings may stand as model systems for the organization of atoms or molecules, or they may be of interest in their own right when canon balls need to be shipped [2,3] or spherical sweets are packed into a jar [4]. Sphere packings have a number of characteristic, density-dependent properties [1]. Of interest in this Letter is the high-density limit in which the spheres ''crystallize'' into hexagonally close-packed structures with a density of 74% [3]. As sketched in Fig. 1, these structures consist of close-packed layers of triangularly arranged spheres [Fig. 1(a)]. At constant density, these can be stacked together in various periodic or random fashions. In the simplest periodic structure, the layers are arranged as *A*-*B*-*A*-*B*-... [Fig. 1(b)], which corresponds to the ''hexagonally close-packed (hcp) structure''. Slightly more complex is the *A*-*B*-*C*-*A*-*B*-*C*-... arrangement [Fig. 1(c)], which corresponds to ''face-centered cubic'' (fcc) structure. All other sequences of these layers are commonly labeled ''random hexagonally close-packed.''

Packing density is generally not the only quantity which a physical system needs to optimize. More intricate physical arguments may select one hexagonally close-packed structure over another, even though they have the same density [5]. This is the case, for example, when the total energy of a packing needs to take into account the presence of long-range interactions between spheres, which is sensitive to the detailed packing structure. Crystallization in strongly charged colloids provides a typical example for this, for which a fcc preference is found [6]. A preference of fcc packing is also regularly reported for truly hard-sphere systems which interact only upon contact or more indirect forces, provided, for example, by the flow of the fluid in which they are dispersed [7,8]. Such hard-sphere systems come in many different types [7–10,10–15], ranging from thermodynamically stable colloids to sedimenting or creaming systems such as foams, emulsions, or granular media. In these systems, fcc preference has been reported, yet has been little investigated and—if at all—tends to be justified by an entropy argument [5]. Whilst the small entropic differences between the structures may account for structural differences in thermodynamically stable colloids [14,15], they seem a less likely candidate to explain fcc preferences in crystals of nearly millimeter-size bubbles [7,13] or granular media [9]. Furthermore, in many of the reported systems, the preference of the fcc packing depends strongly on how the close-packed crystal is generated. Even though this history dependence is a classic feature of a system which undergoes a jamming transition from a less dense to a dense state, it may also be a signature of a mechanical instability, which acts during the crystal formation.

Combining numerical simulations, experiments with equal-volume bubbles, and a simple mechanical argument, we therefore show here that, when hard spheres are packed under an external force field (such as gravity), fcc and other close-packed structures are formed with equal probability. However, the fcc structure is mechanically more stable and therefore less often destroyed in the continuing dynamic process. We demonstrate this here for a particular system

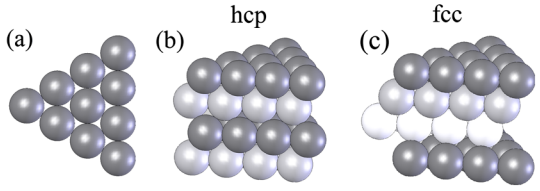

FIG. 1 (color online). (a) Layer of triangularly arranged spheres. (b) *A*-*B*-*A*-*B*-type layering of the hcp, and (c) *A*-*B*-*C*-type layering of the fcc packing, expressed by color coding.

of spheres sedimenting or creaming in a liquid under gravity and steady drainage, but the argument is so elementary that we consider it applicable in much more general scenarios.

The numerical simulations were performed with the in-house code PRIME [16–18], which solves the three-dimensional, incompressible, unsteady Navier-Stokes equations on a Cartesian grid. The spheres are treated by an immersed-boundary method (IBM) which couples the fluid and the moving objects [19], imposing a no-slip condition at their surface. In [18], detailed information on the improved variant of the IBM employed for the present study is available. Some numerical details are also provided in Table I. The motion of the spheres is calculated by solving the differential equation of motion for each sphere. The collision of two spheres, i and j, with center position $\mathbf{X}$, diameter D, and surface tension σ is modeled by an additional repulsive force F_{coll} acting on the center of the spheres in the direction normal to the contact plane

$$F_{\mathrm{coll},i} = \max\{0; 2\pi\sigma(|\mathbf{X}_i - \mathbf{X}_j| - D - r_s)\}. \quad (1)$$

This expression represents the forces which occur upon the deformation of two spheres in contact [20] as with the present IBM forces between surfaces of immersed objects are not resolved. The safety clearance r_s is necessary to prevent the spheres from overlapping and decreases the maximum packing fraction by a small amount ($r_s = 0.1$ D). Tangential collision forces are not explicitly added here because they are not essential for fcc preference [10].

A sketch of the computational setup is shown in Fig. 2(a). It aims to investigate the agglomeration process of spheres on an existing, crystalline sphere cluster which is represented by two layers of fixed, triangularly arranged spheres at the top of the domain. Drainage in the cluster is artificially included by a constant downward velocity v_0 that is imposed at the top of the domain. The horizontal directions are periodic in order to minimize wall and confinement effects on the ordering. The parameters employed in the simulation are given in Table I. They are expressed in terms of the sphere diameter D, fluid density ρ_f, sphere density ρ_p, fluid viscosity ν, static drainage velocity v_0, and the gravitational acceleration g. These parameters correspond to the specific case of small gas bubbles rising in a low-viscosity liquid.

TABLE I. Parameters, similarity numbers, and reference values for the simulations conducted.

Parameter	Symbol	Value
Fixed spheres	$\cdots$	2×56
Mobile spheres	$\cdots$	120
Density ratio	ρ_f/ρ_p	200
Reynolds number	$\mathrm{Re} = \frac{v_0 D}{\nu}$	$4 \cdots 120$
Archimedes number	$\mathrm{Ar} = \frac{(\rho_f - \rho_p) g D^3}{\rho_f \nu^2}$	3.14×10^5
Eötvös number	$\mathrm{Eo} = \frac{(\rho_f - \rho_p) g D^2}{\sigma}$	0.1
Reference length	$L_{\mathrm{ref}} = D$	$\cdots$
Reference velocity	$v_{\mathrm{ref}} = \sqrt{\frac{(\rho_f - \rho_p) g \frac{1}{6}\pi D^3}{\frac{\rho_f}{2}\frac{\pi}{4}D^2}}$	$\cdots$
Reference time	$t_{\mathrm{ref}} = L_{\mathrm{ref}}/v_{\mathrm{ref}}$	$\cdots$
Domain size	$w \times d \times h$	$7\mathrm{D} \times 7\mathrm{D} \times 14\mathrm{D}$
Grid points	$n_w \times n_d \times n_h$	$128 \times 128 \times 256$
IBM marker points	N_L	1056

We released 120 randomly initialized mobile spheres in 100 runs with a rate of $r = 2.5/t_{\mathrm{ref}}$ under a normalized drainage rate v_0/v_{ref}. The spheres rise and agglomerate below the fixed layers. We tested different rates $0.75/t_{\mathrm{ref}} < r < 7.5/t_{\mathrm{ref}}$ without noticing a measurable effect on the results. Figure 2(b) shows how the density profile of the sphere cluster develops as a function of time for $v_0/v_{\mathrm{ref}} = 0.12$. The resulting positions of each sphere in the third and fourth layer were classified into "hcp," "fcc," or "unordered" by matching with the fixed spheres of the

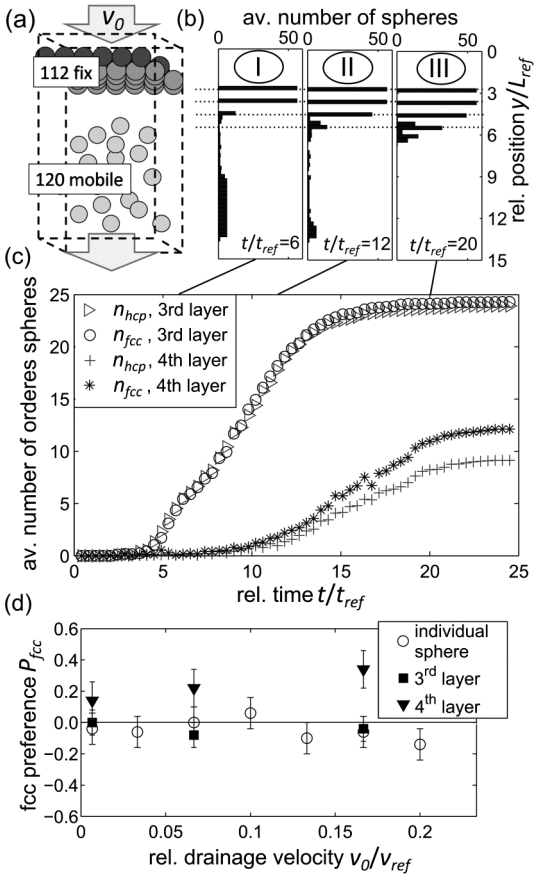

FIG. 2. (a) Setup of the simulations conducted. (b) Averaged distribution of spheres over height at discrete times, showing the filling of the layers. Broken lines indicate the theoretical positions of the ordered layers. (c) Number of ordered spheres n_{fcc} and n_{hcp} in the third and fourth layers averaged over 100 runs. (d) Preference P of fcc ordering in the third and fourth layers and for individual spheres.

first two layers. Figure 2(c) shows how the number n_{fcc} and n_{hcp} of fcc- or hcp-packed spheres, respectively, evolves with time for the third and fourth layer (averaged over 100 runs). We observe three different stages during the process [Figs. 2(b) and 2(c)]: (I) The agglomeration of spheres in the third layer generates fcc or hcp configurations with equal probability [Fig. 2(c)]. (II) The filling of the fourth layer starts before the third layer is complete. There appear slightly more fcc than hcp spheres in the fourth layer. (III) The existing spheres in the fourth layer act as seeds for the arrangement of newly arriving spheres so that the lead of fcc arrangement is amplified even when the third layer is already filled. The equal probability for the occurrence of fcc and hcp configurations in the third layer disproves a previously evoked argument [8] that a fcc preference in bubble clusters may result from the hydrodynamical effects arising when new spheres arrive at an already formed, close-packed cluster. Such an argument assumes that a sphere approaching two closely packed layers (*A*-*B* configuration) may experience less hydrodynamic resistance when approaching in a fcc rather than in a hcp configuration, since the fluid channel above the *C* position of the fcc packing is not blocked by another sphere [Figs. 1(b) and 1(c)]. To further disprove the validity of such an argument, we also performed simulations in which individual spheres arrive on the two fixed layers. To quantify the fcc preference, we define $P_{\mathrm{fcc}} = (n_{\mathrm{fcc}} - n_{\mathrm{hcp}})/(n_{\mathrm{fcc}} + n_{\mathrm{hcp}})$. The fcc preference is plotted against the normalized drainage velocity v_0/v_{ref} in Fig. 2(d). It shows no systematic fcc preference for individual or multiple spheres arriving in the third layer. On the contrary, in the fourth layer P_{fcc} is systematically positive and increases with drainage velocity v_0/v_{ref}. It may be tempting to consider the minimization of the overall hydrodynamic resistance of the close-packed cluster under the imposed drainage as an argument for the dominance of the fcc packing. However, we find that the hydrodynamic resistance of periodic fcc packing is 12% higher than that of hcp packing.

We therefore propose here an alternative argument, which is based entirely on the mechanical stability of the packing: since the third layer is mobile and not completely filled in stage (II), the arrival of spheres in the fourth layer promotes a mechanical instability and rearrangement of the hcp into fcc packing. The drainage flow provides an additional activation energy and therefore leads to an increasing fcc preference. The fundamental mechanism at the heart of this instability is shown in Fig. 3(a). Let us consider a fcc and a hcp pyramid to whose tip we apply an additional force F_{acc} which models accumulated buoyancy or inertial forces of spheres arriving from below. In the fcc pyramid, this force is transferred from sphere (1) over (2) to (3) along a straight contact line. In the hcp pyramid, however, the positions of the sphere centers (1), (2), and (3) are not in line. Thus, the force of sphere (1) transferred to sphere (2), denoted $F_{1,2}$, results in a small outward component F_{out}, which can be calculated as

$$F_{1,2} = \frac{1}{3}\frac{(F_{\mathrm{acc}} + F_b)}{\cos(\vartheta_{1,2})}, \tag{2}$$

$$F_{\mathrm{out}} = F_{1,2}\sin(\vartheta_{1,2} - \vartheta_{2,3}). \tag{3}$$

For sufficiently large F_{acc}/F_b this force can not be compensated by the buoyancy force F_b of sphere (2). Thus, we can state that if $F_{\mathrm{out}} > F_b\sin(\vartheta_{2,3})$, sphere (2) is ejected from the hcp pyramid. This leads to the following stability criterion for the hcp pyramid:

$$\frac{F_{\mathrm{acc}}}{F_b} < \frac{3\sin(\vartheta_{2,3})\cos(\vartheta_{1,2})}{\sin(\vartheta_{1,2} - \vartheta_{2,3})} - 1 \approx 2.0. \tag{4}$$

That is, if $F_{\mathrm{acc}}/F_b > 2.0$, a hcp pyramid is mechanically unstable. We proved this geometrical argumentation by analyzing small hcp and fcc pyramids in numerical simulations as well as in experiments. In the simulations, we placed the pyramids on two layers of fixed spheres and applied different tip forces F_{acc} and drainage velocities v_0. The different regions of stability in relation to the normalized drainage and tip force are shown in Fig. 3(b). Obviously, the fcc pyramid can resist significantly larger tip forces. Drainage decreases the stability of both packings by reducing the effective buoyancy force of sphere (2) until the spheres start to float above $v_0/v_{\mathrm{ref}} \approx 0.23$. The simulated maximum force $F_{\mathrm{acc}}/F_b \approx 1.9$, up to which the hcp pyramid is stable in the absence of drainage is in good agreement with Eq. (4). We have conducted these simulations also with heavy spheres of density ratio $\rho_f/\rho_p \approx 0.1$, yielding similar results.

For experimental investigations [21] we created small monodispersed gas bubbles ($D = 0.9$ mm) in soap solution (''Dreft'') and arranged small pyramids by fixing the first layer in a purpose-shaped frame (triangular for fcc, hexagonal for the hcp pyramid) [Fig. 3(c)]. Bubbles arrive one by one at a frequency of 2.5/s from a nozzle which is placed 4 mm below the pyramid. F_{acc} in this case therefore results from the combined buoyancy and inertial force of an individual bubble arriving at the top of the pyramid. As indicated in the image sequences of Fig. 3(c) and in [21], we find that 90% of the fcc pyramids remain stable while in the hcp configuration the arriving bubble always ejects and replaces a bubble from the second layer. The ejected bubble moves through a valley in the base layer, which is oriented at 180° to the direction of force $F_{1,2}$.

To follow such processes within much larger sphere clusters, we analyze the rearrangement of spheres during the compaction process in the full-scale simulations. In plotting the angle of ejection Φ, Fig. 4(a) shows that spheres in the third layer are regularly ejected from their positions in the packing and that they move with roughly equal probability through one of the three valleys created by the second layer. To distinguish more accurately the

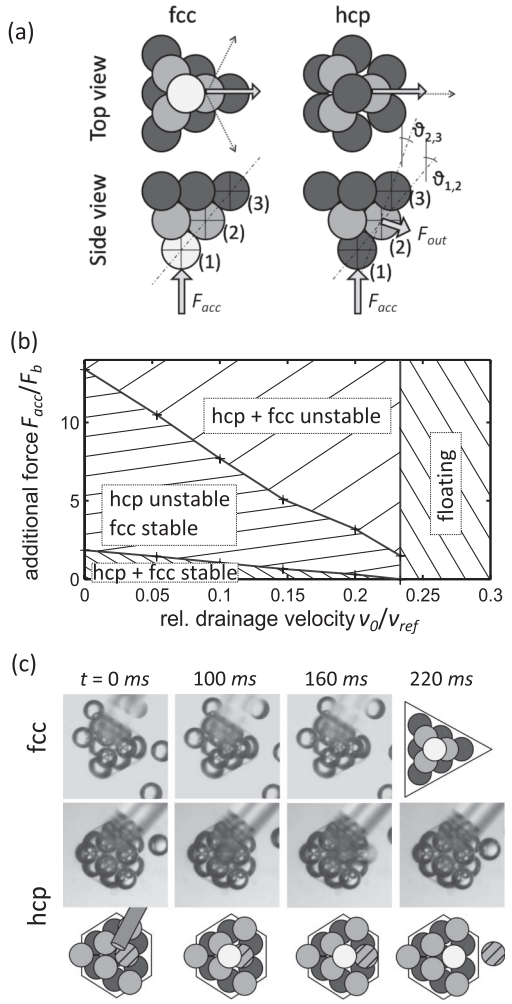

FIG. 3. (a) Geometrical situation and force transfer in fcc and hcp with coloring as in Fig. 1. (b) Stability map of the fcc and hcp pyramid under tip force and drainage. (c) Experimental observation of stable fcc and the rearranging hcp pyramids of bubbles.

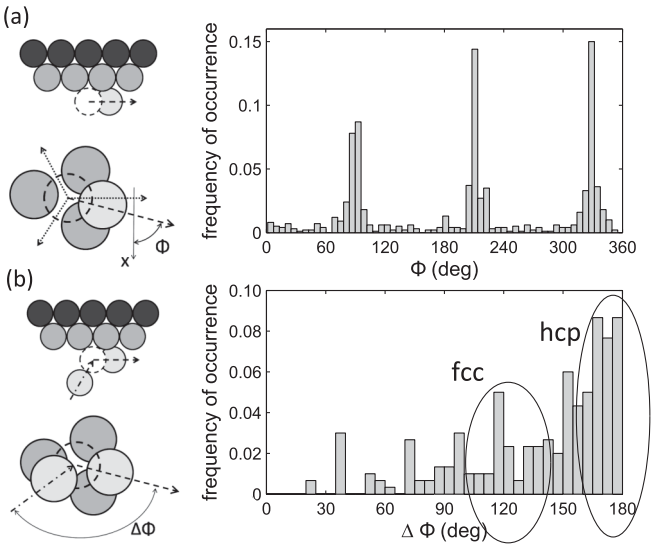

FIG. 4. (a) Frequency of occurrence of the angle between the x direction and path of permanently ejected spheres (dashed arrow) in layer three. The three dominant angles correspond to the three valleys in layer two, identified by three dotted arrows. (b) Frequency of occurrence of the angle between the ejecting path (dashed arrow) and direction of force (dash-dotted arrow) exerted from the sphere from the fourth layer on the ejected sphere in the third layer.

type of rearrangements, Fig. 4(b) presents the relative angle $\Delta\Phi$ between the direction of ejection and the force $F_{1,2}$ exerted from a sphere in the fourth layer onto a sphere in the third layer. $\Delta\Phi = 180°$ indicates rearrangement in hcp packing, while $\Delta\Phi = 120°$ is a signature of rearrangements in fcc packing. The dominance of hcp-type rearrangements is very clear, leading to the pronounced fcc preference in the fourth layer.

In conclusion we propose that the following mechanism may be at the origin of the repeated observation of a fcc preference in a wide range of hard-sphere systems: During the packing process, small fcc and hcp elements continuously form with equal probability. However, under the impact of newly arriving spheres, the hcp elements are destroyed more frequently than the fcc elements due to their lower mechanical stability. This argument may play a central role in any packing process which provides sufficient activation forces, time, and room for such rearrangements to occur. It may therefore also explain why the question of fcc dominance is so dependent on the type of sphere system and its packing history [10]. Full-blown simulations, like the ones performed in the present study, should not be necessary to evidence this phenomenon. In our case, we needed the presence of the fluid in order to discard some of the regularly raised hydrodynamic arguments for a fcc preference. Up until now we have not discussed the influence of tangential friction between the spheres, composed of fluid friction and static friction directly between the spheres. Fluid friction only acts on moving spheres and therefore cannot stabilize a statically unstable configuration. However, it may significantly slow down the ejection of sphere (2) and therefore influence the final fcc preference due to the packing dynamics. Static friction, on the other hand, could counter F_{out} and thus stabilize both packings. This should be the case, in particular, for solid grains and could be overcome by shaking [9] or shear [11]. We have done very simple experiments on pyramids of metal spheres [21] with tangential friction. We find that a fcc pyramid can stand $F_{\text{acc}}/F_b \geq 1500$ while a hcp pyramid collapses at $F_{\text{acc}}/F_b \leq 15$. As far as we are aware, the significant difference of the mechanical stability of fcc and hcp elements has never been evoked in the literature. The importance of this fact may well go beyond questions of fcc preference and it may turn the packing of spheres more into a science than an art.

We acknowledge Tobias Kempe and Stephan Schwarz for their contribution to the development of the code PRIME, Dominique Langevin for facilitating a one-year

stay for S. Heitkam in her group where part of this work was performed, as well as D. Weaire, S. Hutzler, and R. Höhler for many fruitful discussions. This work was financed by a DFG grant (SFB609) and by the French Ministry of Foreign and European Affairs (''Eiffel'' programme).

[1] D. A. Weitz, Science **303**, 968 (2004).
[2] J. Kepler, *Strena seu de Nive Sexangula* (Godefridum Tampach, Francofurti ad Moenum, 1611).
[3] T. C. Hales, Discrete & Computational Geometry **36**, 5 (2006).
[4] T. Aste and D. Weaire, *The Pursuit of Perfect Packing* (Institute of Physics, Bristol, UK, 2000).
[5] L. V. Woodcock, Nature (London) **385**, 141 (1997).
[6] J. P. Hoogenboom, A. Yethiraj, A. K. van Langen-Suurling, J. Romijn, and A. van Blaaderen, Phys. Rev. Lett. **89**, 256104 (2002).
[7] A. van der Net, W. Drenckhan, I. Weaire, and S. Hutzler, Soft Matter **2**, 129 (2006).
[8] A. van der Net, G. W. Delaney, W. Drenckhan, D. Weaire, and S. Hutzler, Colloids and Surfaces A **309**, 117 (2007).
[9] A. B. Yu, X. Z. An, R. P. Zou, R. Y. Yang, and K. Kendall, Phys. Rev. Lett. **97**, 265501 (2006).J. A. Rodrigues, E. Rio, J. Bobroff, D. Langevin, and W. Drenckhan, Colloids and Surfaces A **384**, 408 (2011).
[10] A. J. Meagher, M. Mukherjee, D. Weaire, S. Hutzler, J. Banhart, and F. Garcia-Moreno, Soft Matter **7**, 9881 (2011).
[11] W. Loose and B. J. Ackerson, J. Chem. Phys. **101**, 7211 (1994).
[12] J. R. Huang and T. G. Mason, Soft Matter **5**, 2208 (2009).
[13] R. Höhler, Y. Y. C. Sang, E. Lorenceau, and S. Cohen-Addad, Langmuir **24**, 418 (2008).
[14] F. Ramiro-Manzano, F. Meseguer, E. Bonet, and I. Rodriguez, Phys. Rev. Lett. **97**, 028304 (2006).
[15] H. Miguez, F. Meseguer, C. Lopez, A. Mifsud, J. S. Moya, and L. Vazquez, Langmuir **13**, 6009 (1997).
[16] T. Kempe and J. Fröhlich, in 7th International Conference on Multiphase Flow, Tampa, Florida, 2010 (unpublished).
[17] T. Kempe and J. Fröhlich, in 8th International ERCOFTAC Symposium on Engineering Turbulence Modelling and Measurements, Marseille, France, 2010 (unpublished).
[18] T. Kempe and J. Fröhlich, J. Comput. Phys. **231**, 3663 (2012).
[19] M. Uhlmann, J. Comput. Phys. **209**, 448 (2005).
[20] See Supplemental Material at http://link.aps.org/supplemental/10.1103/PhysRevLett.108.148302 for derivation.
[21] See Supplemental Material at http://link.aps.org/supplemental/10.1103/PhysRevLett.108.148302 for experimental details.